Physics of the Earth and Planetary Interiors, 49 (1987) 30–36
Elsevier Science Publishers B.V., Amsterdam – Printed in The Netherlands

Monte-Carlo simulation of record envelope of a near earthquake

A.A. Gusev and I.R. Abubakirov

Institute of Volcanology, Petropavlovsk-Kamchatskiy, 683006 (U.S.S.R.)

(Received September 12, 1986; revision accepted December 2, 1986)

Gusev, A.A. and Abubakirov, I.R., 1987. Monte-Carlo simulation of record envelope of a near earthquake. Phys. Earth Planet. Inter., 49: 30–36.

It is difficult to calculate analytically envelopes of scattered seismic waves from a near earthquake for a simple and important model of multiple anisotropic scattering in homogeneously scattering space. Monte-Carlo simulation was carried out for the acoustic case; as a first approximation its results can be used to describe S waves and coda of a near earthquake.

By means of simulation we can imitate the following features of real envelopes: (1) lack of short initial S-pulse with 'source' duration at dimensionless distances $\rho \geqslant 1$; (2) amplitude attenuation of S waves that is considerably more rapid than the inverse distance law. The result agrees well with the diffusion model; therefore we can suggest a universal asymptotic coda shape function.

1. Introduction

No perfectly adequate models are proposed to date for a theoretical description of a record of a near earthquake. After studies by Aki (1969) and Aki and Chouet (1975) it became clear that the general concept of 'direct' wave scattering on random heterogeneities of the medium is applicable. In frames of the simplest model of single isotropic scattering Aki and Chouet (1975) described coda, and Kopnichev (1975) and Sato (1977) described envelope shape after the 'direct arrival'. Envelope shape in this model was distance-independent (after scaling). Kopnichev (1977) proposed formulas for contributions of double and triple scattering. Sato (1984) took into account the source directivity function for S waves. Gao et al. (1983) proposed formulas to account for multiple-scattered body waves up to multiplicity 7, and also the approximate asymptotic formula.

Anisotropy of scatterers (for single scattering) was taken into account by Sato (1984). Several studies considered conversion scattering, and the scattering on the heterogeneities that were considered directly as some random field of perturbations of medium density and elastic moduli (Sato, 1984; Malin and Phinney, 1985, etc.). We shall, however, consider only more primitive phenomenological description of the scattering process.

As a whole, for sufficiently small distances and elapse times, until the single scattering model is valid, a rather full model is developed. For typical mean free path value $l = 100$ km, 'small' means distances up to 30–50 km and elapse times up to 10–20 s. For greater distances and elapse times the adequate model is lacking, and the diffusion model (Aki and Chouet, 1975) is not applicable to describe near earthquake records in this domain.

As mentioned by Gusev and Lemzikov (1983, 1985), the isotropic scattering model predicts qualitatively inaccurate record shape: according to this model, a short direct body wave pulse (with 'source' duration) must be observed up to distances $r = (2–3)l$. In fact, this pulse, if observed, can be seen only at distances of 10–30 km, seldom at 50 km, or $(0.1 - 0.5)l$. This contradiction was

0031-9201/87/$03.50

ascribed to the effect of anisotropy of scattering in the real Earth, and a simple model was proposed, as a combination of isotropic and 'Gaussian' indicatrices. In the same study the diffusion model was proposed to be used as a provisional 'interpolation model' between domains of validity of single-scattering (Born) and diffusion approximations. Many of the qualitative considerations of the studies by Gusev and Lemzikov (1983, 1985) shall be more strongly grounded in the following.

2. Technique of simulation

Essentially, we simulated here the Green's function of the non-stationary radiation transport equation for scalar waves. The usual analogy was used between propagation of particles and wavelets with random phases, and the classical Monte-Carlo method, well known in neutron physics or in atmospheric optics, was used. It was realized in the following way. Simulated particles were repeatedly emitted from a fixed point source, then they propagated through space with simulated random point scatters (a new set of scatterers was generated for each trajectory). Positions of each particle were determined with constant time step, and distance from the source was computed. Pairs (time, distance) were recorded in a 2D histogram; to do this, distance values were quantified with the distance step equal to $2 \times$ time-step $\times$ velocity. Values of distance and time steps determine the resolution of obtained envelope curves. The standard size of the histogram, 70 time by 20 distance units, giving 1400 space-time compartments (cells), was always used. Therefore potential receiver points within a spherical shell of the thickness of one distance unit were represented by one distance interval, and the history of the number of particles in this shell was recorded in one column of the histogram table.

The simulated particle trajectories were 3D broken lines consisting of several straight segments. Each moving simulated particle was 'observed' during all 70 time steps; either it left the largest spherical shell or it did not (it could return). For each segment, its length L was random and was drawn from the same exponential distribution with density

$$p(L/l) = \exp(-L/l)/l$$

This means that the probability of scattering is constant for any unit volume. As for the direction of a segment, it was spherically isotropic random for the first segment. For other segments, direction was either also isotropic or anisotropic according to the accepted indicatrix function for a given simulation run. Let θ be the angle of scattering, i.e. the angle between two successive segments of a trajectory considered as vectors. In the anisotropic case, the random number θ was generated according to Rayleigh's density function (producing 'Gaussian' indicatrix)

$$p(\theta) = a\theta \exp(-\theta^2/2\,\delta^2) \qquad (1)$$

where the parameter δ determines the angular width of the indicatrix. The δ value was constant for a given simulation run.

After monitoring a sufficient number of trajectories, the accumulated number in each cell of the histogram was divided by the number of all trajectories/particles and by the volume of the above-mentioned spherical shell giving a Monte-Carlo estimate of energy density (per unit energy radiated). We assumed the particle/wave velocity as constant and equal to unity; in this case the energy density is equal to the mean spherical (omnidirectional) radiation intensity. After this transformation, each column of the table represents the time history of radiation intensity at a certain distance, and each row of the table represents the distance dependence of radiation intensity at a moment of time. The mean free path value was also accepted to be unity during simulation. Therefore our results were obtained (and are presented below) as functions of dimensionless distance $\rho = r/l$ and dimensionless time $\tau = ct/l$, where c is the wave velocity. Observational data should be converted to these scales to be comparable to the results of simulation.

Anelastic energy loss was not simulated, but it can be easily accounted for when the quality factor Q is constant everywhere: the simulated intensity function should be multiplied by $\exp(-2\pi ftQ^{-1})$. The simulation results are valid for the whole space; they are applicable also to the

half-space with a mirror boundary, when the source is near the boundary and the receiver is on it.

3. Isotropic case

To model the isotropic case is important from several points of view:

(1) this is the basic, theoretically simplest case, and, when $\tau \ll 1$, analytical results are known.

(2) Different formulas were proposed to correct single-scattering results for contribution of multiple scattered energy.

(3) Different opinions on the applicability of diffusion approximation: (a) at $\tau \gg 1$ and (b) at $\tau = 1 - 3$.

In Fig. 1, the simulated asymptotic ($\tau \gg \rho$, coda) envelope shape is presented in wide and narrow elapse time ranges. In Fig. 2, examples of simulated envelopes are given. Inspection of Fig. 1 leads to the following conclusions:

(1) Kopnichev's (1977) formula for coda (multiplicities 1, 2, and 3) is valid for $\tau \lesssim 0.1$ and the

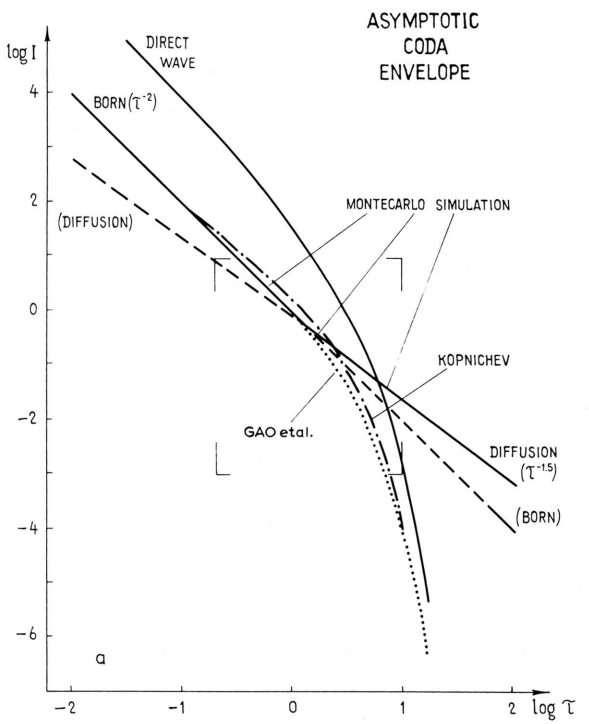

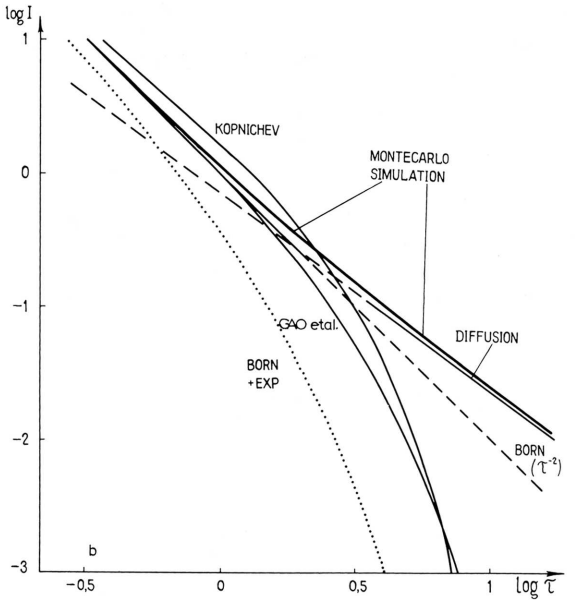

Fig. 1. Asymptotic intensity functions for scattered waves (case $\tau \gg \rho$, coda). (a) in wide, (b) in narrower τ range. Dimensionless absolute level of curves is determined by assuming: source energy = 1, velocity $c = 1$, mean free path $l = 1$. Direct wave intensity function $\rho^{-2} \exp(-\rho)$ is plotted also, for distance $\rho = \tau$. Born case is the function $(2\pi\tau^2)^{-1}$, diffusion case is the function $((4\pi/3)\tau)^{-3/2}$, 'Born + exp' case is the function $(2\pi\tau)^{-1} \exp(-\tau)$, for Kopnichev and Gao formulas for multiple body wave scattering see (Kopnichev, 1977) and (Gao et al., 1983). Simulation results coincide with their approximation by eq. 2. Note that both formulas for multiple scattering were introduced by their authors as corrections to the 'Born + exp' case and not to the 'Born' case. So there is no contradiction when corresponding curves are below the level of the 'Born' curve.

formula of Gao et al. (1983) (multiplicities up to 7) is valid for $\tau \lesssim 0.6$. The best and the simplest approximation for $\tau \lesssim 0.6$ seems to be the initial Born approximation (without $\exp(-\tau)$ factor). This confirms the guess of Aki and Chouet (1975) that a decrease in the level of single scattered waves is compensated (in fact, overcompensated) by an increase in the level of multiple scattered ones.

(2) The analytical formula of Kopnichev (1975) and Sato (1977) for the single-scattered envelope model is applicable up to $\rho \approx 0.5$ and becomes qualitatively invalid at $\rho > 1$.

(3) The diffusion approximation gives an accu-

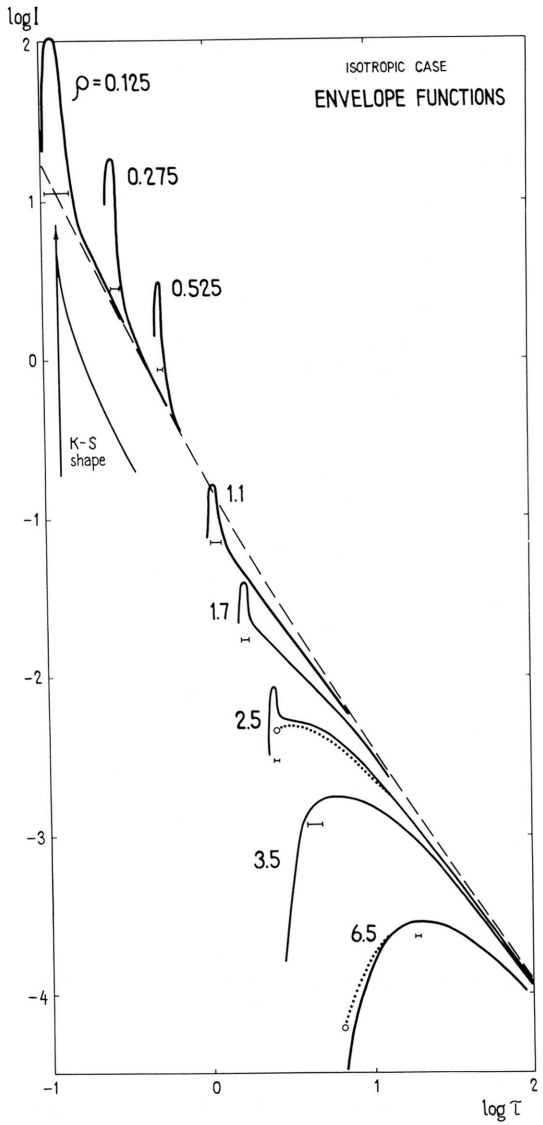

Fig. 2. Examples of simulated intensity functions for isotropic scattering case, for different ρ values. The level of curves is as in Fig. 1. Horizontal bars denote the size of the space-time compartment used in the course of simulation of the individual curve. By dotted lines, diffusion approximation $(4\pi\tau/3)^{-3/2}$ $\exp(-\rho^2/(4\tau/3))$ is shown for corresponding ρ, for $\tau > \rho$. $K-S$ is the intensity function of (Kopnichev, 1975) and (Sato, 1977) for single scattering plotted at an arbitrary level. Its shape does not depend on ρ in bilog scale; it is given by $x^{-1}\ln((x+1)/(x-1))$ where $x = \tau/\rho$. The dashed line corresponds to eq. 2.

rate coda asymptote at $\tau \gtrsim 3$; at $\rho \geqslant 2$ it predicts qualitatively the whole envelope function shape (at $\tau > \rho$), except for an initial delta-like pulse (the reality of which is doubtful for the Earth).

(4) In accordance with the guess of Gusev and Lemzikov (1983, 1985), the coda envelope asymptote ($\tau \gg \rho$) between $\tau = 0.1$ and $\tau = 3$ smoothly changes its slope from -2 (Born approximation) to -1.5 (diffusion approximation). (The level of the diffusion branch on the plots of Gusev and Lemzikov (1983, 1985) is in error which is corrected here, see Fig. 1.) To describe the smooth asymptote of Fig. 1, a universal approximating function is fitted, which is valid for any $\tau \gg \rho$ with an accuracy of $\sim 10\%$ or better

$$I(\tau) = \frac{k^2\left(1 + (k\tau)^{1.85}\right)^{1/3.7}}{2\pi(k\tau)^2} \qquad (2)$$

where $k = 27/16\pi \approx 1/1.86$.

4. Anisotropic case

Modelling of the anisotropic case for a homogeneous medium was undertaken with the following aims in mind:

(1) to find out if it is possible to obtain in frames of the accepted model a set of envelope functions which are in qualitative agreement with the observed ones.

(2) If this is possible, to determine the probable value of the parameter δ of a law (1).

Simulation was carried out for $\delta = 25°$, then after analysis we choose the value $\delta = 50°$ which was considered acceptable as a realistic one. The results are seen in Fig. 3, their inspection shows the following:

(1) 'Narrow' (25°) indicatrix leads to the pronounced decrease of intensity just after the main 'direct wave' wavelet. At $\rho \approx 0.3$ and $\tau \approx 1$ intensity falls definitely below asymptotic (coda) level. This phenomenon is not observed really (Rautian et al., 1981). In the model it is produced by the low probability of multiple back scattering just after the moment when wavelets pass by the receiver point. When $\delta = 50°$ was chosen, this detail of the curves disappears. In both cases pulse

widening with distance is observed, and 'direct wave' pulse becomes less and less clear at $\rho = 0.8 - 1.2$. Thus, the main qualitative features of real records are modelled in this case.

(2) In Gusev and Lemzikov (1983) it was supposed that diffusion approximation must also be valid in the anisotropic case, and that for numerical agreement one should substitute the l value in diffusion law by $l_{IS} = ct_0$, where t_0 is 'isotropization time'. The ratio $l_{IS}/l = N_0$ is the number of scattering acts which is needed for a particle to forget its initial direction. For the Gaussian indicatrix it was speculated that N_0 is proportional to δ^{-2}. These guesses were confirmed by simulation, and approximate formula can now be proposed

$$l_{IS}/l \approx 1.3/\delta^2$$

Therefore, not relating the general question of applicability of diffusion theory to the real Earth, we may note that theoretical grounds for such an application are present even in the case of anisotropic scattering.

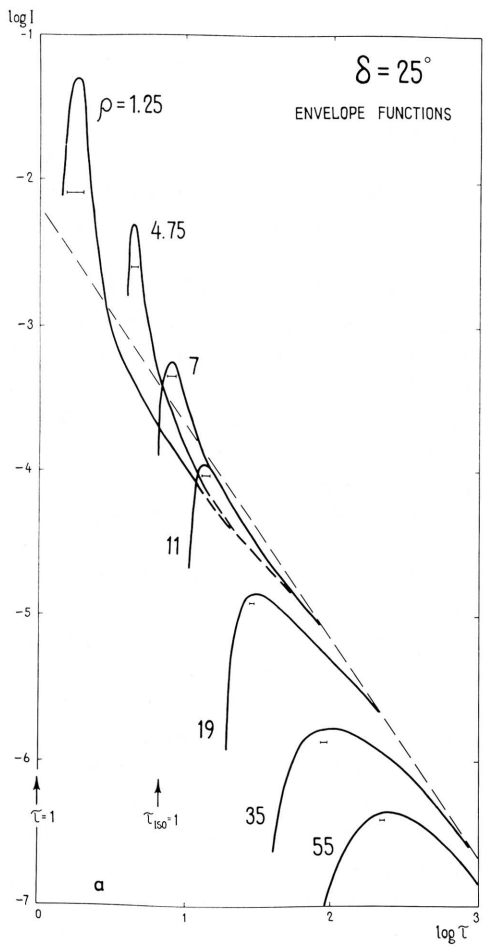

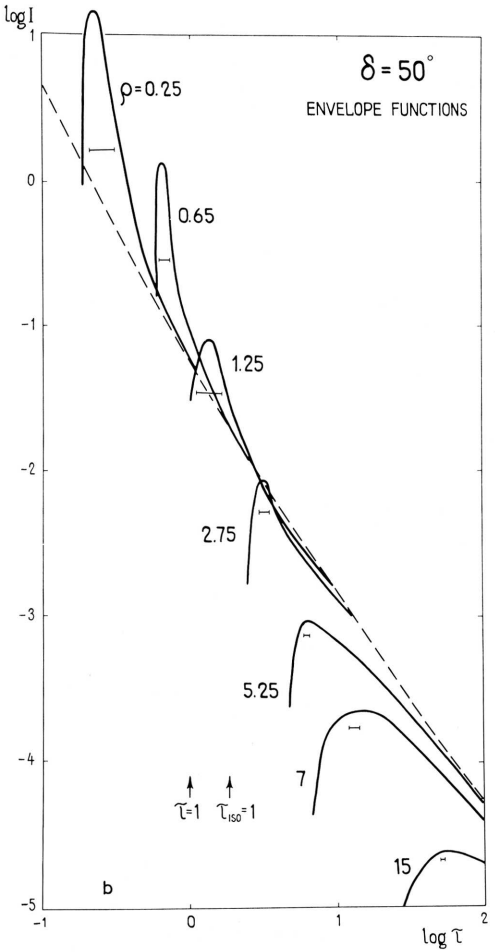

Fig. 3. Examples of intensity functions for anisotropic scattering case, for $\delta = 25°$ (a) and $50°$ (b). See Fig. 2 for explanation.

(3) Let us use the l_{IS} as the new distance unit, let $\rho_0 = r/l_{IS}$ and $\tau_0 = t/t_0$ in a similar way. As was mentioned in Gusev and Lemzikov (1983, 1985), for $\rho > 1$ and $\rho_0 \ll 1$, the width of the 'direct' wave pulse grows as ρ^2, but its energy is nearly the same as that without scattering, so that amplitude decreases as ρ^{-2}. For $\delta = 25°$, when $l_{IS}/l = N_0 \approx 6$, this amplitude trend is seen even up to $\rho = 30$ ($\rho_0 \approx 5$).

(4) We can now suppose that experimental de-

termination of the mean free path l_{ob} from coda yields l_{IS} (and not l). Let $l_{ob} = 100$ km for rough estimates (Sato, 1977). Now we can determine the

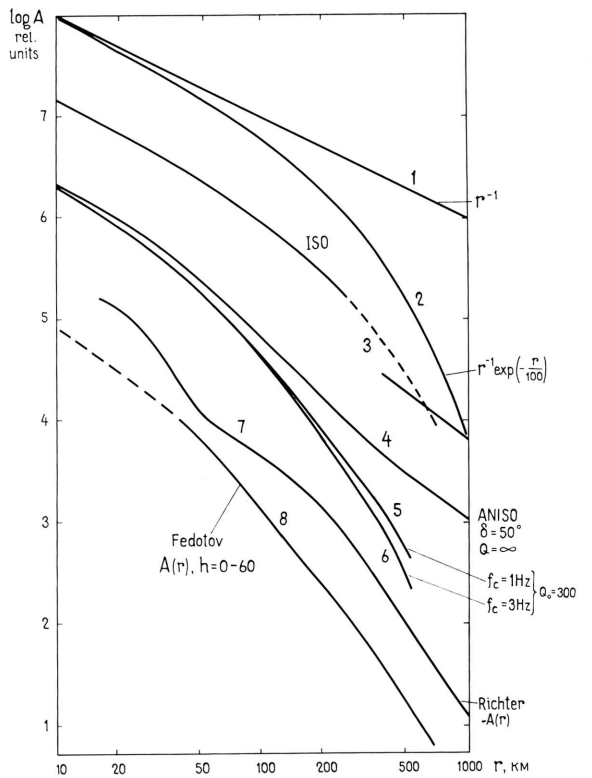

Fig. 4. Amplitude attenuation laws in the distance range $r = 10 - 1000$ km. Assumed $c = 3.5$ km s^{-1} and $l = 100$ km, so the distance range is $0.1 - 10$ for ρ or ρ_0. The upper two curves correspond to homogeneous medium and to the 'pure' direct wave in isotropically scattering medium ($\rho^{-1} \exp(-\rho/2)$. The third curve is the simulated amplitude for the isotropic case corrected for source duration $d = 1$ s. It consists of a 'direct' branch practically coinciding with the second curve and the 'diffusion' branch with slope -1.5. The position of the point of branch intersection is defined by the ratio l/cd. Upper in the next bunch of curves is the simulated amplitude for anisotropic ($\delta = 50°$) case, again corrected for $d = 1$ s, with $l_{IS} = 100$ km. The lower two curves represent the effect of anelastic absorption. We assumed S-wave source with ω^{-2} spectrum and corner frequencies 1 (upper) or 3 Hz (lower curve), corresponding roughly to $M_L = 4$ or $M_L = 2$ earthquakes. Medium properties: $Q = 300\ f^{-0.5}$. Receiver: standard Wood–Anderson seismograph. The lowest two curves are Richer's calibration curve for California converted to r argument, and Fedotov's (1972) S-wave amplitude curve for Kamchatka (depth 0–60 km, for electromagnetic seismograph with $T_S = 1.2$ s). For rough estimates, one can neglect the difference between the recording instruments for Kamchatka and California.

exponent n of amplitude attenuation law $A \sim r^{-n}$. The distance interval was accepted as $r = 20$–300 km, and the direct pulse duration at $r = 0$ km was accepted as 1 s. For the isotropic case we obtain $n = 1.50$ (duration is constant in this case). For the anisotropic case, for both $\delta = 25°$ and $\delta = 50°$, $n = 1.85$. If in this case one takes anelastic loss into account (let $Q = 300\ f^{0.5}$ and source corner frequency 1 and 3 Hz) then the n value increases up to 2.05–2.24. This value is in good agreement with the slope of short-period amplitude curves (of Richter, Fedotov, etc.) in this distance interval, see Fig. 4. Therefore, the model of multiple anisotropic scattering provides a theoretical basis for amplitude attenuation curves of near earthquakes.

5. Conclusion

(1) Monte-Carlo simulation is an efficient means to obtain theoretical envelope shapes of near earthquakes.

(2) The isotropic scattering model gives qualitatively inaccurate envelopes around the arrival time. For asymptotic case (coda), a universal envelope function is proposed which is valid for any dimensionless lapse time.

(3) The anisotropic scattering model with a Gaussian indicatrix of width 50° which enhances forward scattering produced envelopes that appeared to be realistic.

(4) The diffusion approximation is applicable for large elapse times in the isotropic case and can be modified for the anisotropic case; it gives qualitatively reasonable envelopes for large elapse times.

(5) The anisotropic scattering model predicts realistic amplitude attenuation curves for small near earthquakes.

References

Aki, K., 1969. Analysis of the seismic coda of local earthquakes as scattered waves. J. Geophys. Res., 74: 615–631.

Aki, K. and Chouet, B., 1975. Origin of coda waves: source, attenuation and scattering effects. J. Geophys. Res., 80: 3322–3342.

Gao, L.S., Biswas, N.N., Lee, L.C. and Aki, K., 1983. Effects of multiple scattering on coda waves in 3D medium. Pageophys., 121: 3–15.

Gusev, A.A. and Lemzikov, V.K., 1983. Estimation of shear wave scattering characteristics in crust and upper mantle of Kamchatka from observations of Shipunsky station. Volcanol. Seismol., 1: 96–107.

Gusev, A.A. and Lemzikov, V.K., 1985. Properties of scattered elastic waves in the lithosphere of Kamchatka: parameters and temporal variations. Tectonophysics, 112: 137–153.

Kopnichev, Yu.F., 1975. A model of formation of the tail part of a seismogram. Doklady AN SSSR, 222: 333–336.

Kopnichev, Yu.F., 1977. On the role of multiple scattering in formation of the tail part of a seismograms. Izv. AN SSSR, Fizika Zemli, 6: 41–48.

Malin, P.E. and Phinney, R.A., 1985. On the relative scattering of P and S waves. Geophys. J. R. Astron. Soc., 80: 603–618.

Rautian, T.G., Khalturin, V.I., Zakirov, M.S., Zemtsova, A.G., Proskurin, A.P., Pustovitenko, B.G., Pustovitenko, A.N., Sinelnikova, L.G., Filina, A.G. and Shengelia, I.S., 1981. Experimental Studies of Seismic Coda. Nauka, Moscow, 142 pp.

Sato, H., 1977. Energy propagation including scattering effect: single isotropic scattering approximation. J. Phys. Earth., 25: 27–41.

Sato, H., 1984. Attenuation and envelope formation of three-component seismograms of small local earthquakes in randomly inhomogeneous lithosphere. J. Geophys. Res., 89: 1221–1241.